

Short Note

Ethyl 1-Butyl-2-(2-hydroxy-4-methoxyphenyl)-1H-benzo[d]imidazole-5-carboxylate

Reshma Sathyanarayana and Boja Poojary *

Department of Chemistry, Mangalore University, Mangalagangothri, Mangaluru 574199, Karnataka, India; s.reshma1091@gmail.com

* Correspondence: bojapoojary@gmail.com; Tel.: +91-944-886-5403

Abstract: Ethyl 4-(butylamino)-3-nitrobenzoate upon “one-pot” nitro-reductive cyclization using sodium dithionite and substituted aldehyde in dimethyl sulphoxide affords ethyl 1-butyl-2-(2-hydroxy-4-methoxyphenyl)-1H-benzo[d]imidazole-5-carboxylate in an 87% yield. The structural characterization was determined by Fourier-transfer infrared spectroscopy (FT-IR), Proton nuclear magnetic resonance ($^1\text{H-NMR}$), Carbon-13 nuclear magnetic resonance ($^{13}\text{C-NMR}$), mass spectrometry, Ultraviolet-visible(UV-Vis), photoluminescence (PL), thin-film solid emission spectra, cyclic voltammetry (CV) and thermogravimetric (TGA) analysis. Molecular electrostatic potential (MEP) was studied to determine the reactive sites of the molecule.

Keywords: benzimidazole; nitro-reductive cyclization; UV-Vis; photoluminescence; CV; TGA



Citation: Sathyanarayana, R.; Poojary, B. Ethyl 1-Butyl-2-(2-hydroxy-4-methoxyphenyl)-1H-benzo[d]imidazole-5-carboxylate. *Molbank* **2021**, *2021*, M1192. <https://doi.org/10.3390/M1192>

Academic Editors: Panayiotis A. Koutentis and Andreas S. Kalogirou

Received: 29 January 2021
Accepted: 22 February 2021
Published: 24 February 2021

Publisher's Note: MDPI stays neutral with regard to jurisdictional claims in published maps and institutional affiliations.



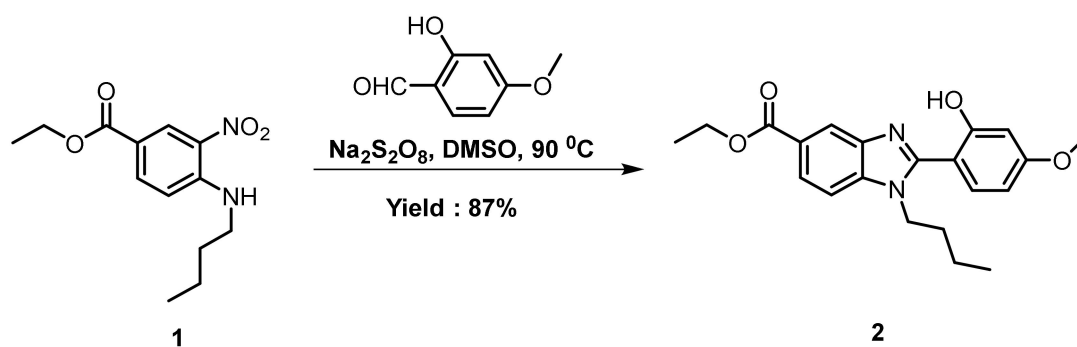
Copyright: © 2021 by the authors. Licensee MDPI, Basel, Switzerland. This article is an open access article distributed under the terms and conditions of the Creative Commons Attribution (CC BY) license (<https://creativecommons.org/licenses/by/4.0/>).

1. Introduction

Benzimidazole and its derivatives are well documented in the literature, with varied biological properties [1–6]. Interestingly, a great work on benzimidazole in the field of optoelectronic [7–15] is also known, as these moieties possess a fluorescent property. The organic solid-based luminescent materials have received enormous attention due to their varied application in organic photovoltaics [16], sensors [17], organic field-effect transistors [18], organic lasers [19] and organic light-emitting diodes [20]. A tremendous effort has been made in the field of organic light emitting diodes (OLEDs) due to their huge application in lighting and display [21]. Despite the successful application of OLEDs in solid-state lighting and flat-panel display, some of the fault-findings, such as the efficiency of electroluminescence, manufacturing cost and stability [22], still need to be resolved. For practical applications, luminophores are normally used in solid-state films. Discovering a novel blue-emitting device remains a subject of interest, as full-color displays depend on red, green and blue (RGB) emission [23]. As such, we report on the synthesis and optoelectronic properties of title compound **2** as the blue-emitting material.

2. Results

The title compound **2** was prepared following the procedure reported in the literature [24]. The nucleophilic substitution for ethyl 4-chloro-3-nitrobenzoate yields 4-(butylamino)-3-nitrobenzoate **1**. Upon adding substituted salicylaldehyde and sodium dithionite to compound **1** in DMSO, compound **1** undergoes a “one-pot” nitro reductive cyclization to achieve target compound **2** in an 87% yield, as an off-white solid (Scheme 1). The structural support for the compound was provided by elemental analyses, FT-TR, $^1\text{H-NMR}$, $^{13}\text{C-NMR}$ and mass spectrometry (Supplementary Materials).



Scheme 1. Synthesis of ethyl 1-butyl-2-(2-hydroxy-4-methoxyphenyl)-1H-benzo[d]imidazole-5-carboxylate (**2**).

3. Discussion

The FT-IR spectrum of the final compound **2** displayed a broad peak at 3412 cm^{-1} , which confirms the presence of the OH group. In addition, a sharp band at 1701 cm^{-1} corresponds to C=O stretching. In the ^1H NMR spectrum the presence of the butyl group was supported by the appearance of a triplet, quartet, quintet and triplet at 0.74, 1.13, 1.64 and 4.28 ppm, respectively, whereas the ethyl group was confirmed by the presence of a triplet and quartet at 1.36 and 4.35 ppm, respectively. The methoxy protons resonated at 3.86 ppm. The six aromatic protons appeared in the region 6.66–8.26 ppm. The successful design of final compound **2** was also supported by a COSY experiment, which evidenced a correlation between the methylene and methyl groups. In the ^{13}C NMR spectrum a characteristic peak at 166.1 corresponds to carbonyl carbon of ester. The remaining aromatic and aliphatic carbon signals appeared in the expected region. Further, in the mass spectrum, a molecular ion peak appeared at an m/z value of 369.15 [MH^+] in the positive ionization mode.

3.1. UV-Vis Absorption and Photoluminescence (PL) Properties

The optical properties of the target molecule **2** were determined at room temperature, with a set concentration of $2\text{ }\mu\text{M}$ solution in acetonitrile (Figure 1). The title compound displayed three major absorption bands at 229, 262 and 326 nm. The fluorescence spectra exhibited dual emissions at 369 nm (i.e., weak sub-band) and 429 nm (i.e., strong main band) in acetonitrile solvent at $2\text{ }\mu\text{M}$ concentration due to phototautomerization [12] (Figure 1). The compound **2** displayed 103 nm of Stokes shift. In addition, the compound exhibited high fluorescence in the spin-coated solid film, with emission maxima 460 nm (Figure 1). The solid-state emission peak of compound **2** was red-shifted to 31 nm when compared to that of the solution state. The fluorescence quantum yield (Φ_f) of the solution gave the value of 0.10 using Equation (1).

$$\Phi = \Phi_R \frac{I}{I_R} \frac{\text{OD}_R}{\text{OD}} \frac{n^2}{n_R^2} \quad (1)$$

where I is the integrated intensity, OD is the optical density and n is the refractive index, and the subscript R refers to the reference fluorophore of known quantum yield [25].

3.2. Electrochemical Properties

The cyclic voltammetry was performed to probe the electrochemical properties and energy levels of synthesized molecule **2** in a chloroform solution. The compound exhibited one onset oxidation potential in the anodic region at 0.97 (Figure 2). The energy level of the highest occupied molecular orbital ($E_{\text{HOMO}} = -[E_{\text{onset}}^{\text{ox}} + 4.8\text{ eV} - E_{\text{FOC}}]$) of the title compound was found to be -5.49 eV , whereas the lowest unoccupied molecular orbital ($E_{\text{LUMO}} = E_{\text{HOMO}} + E_g$) was -1.99 , which was determined by onset oxidation potential ($E_{\text{onset}}^{\text{ox}}$) and optical band gap ($E_g = \frac{1240}{\lambda_{\text{onset}}}$), where λ_{onset} is the onset absorption. The energy gap between HOMO and LUMO ($\Delta E = \text{HOMO} - \text{LUMO}$) is calculated to be 3.50.

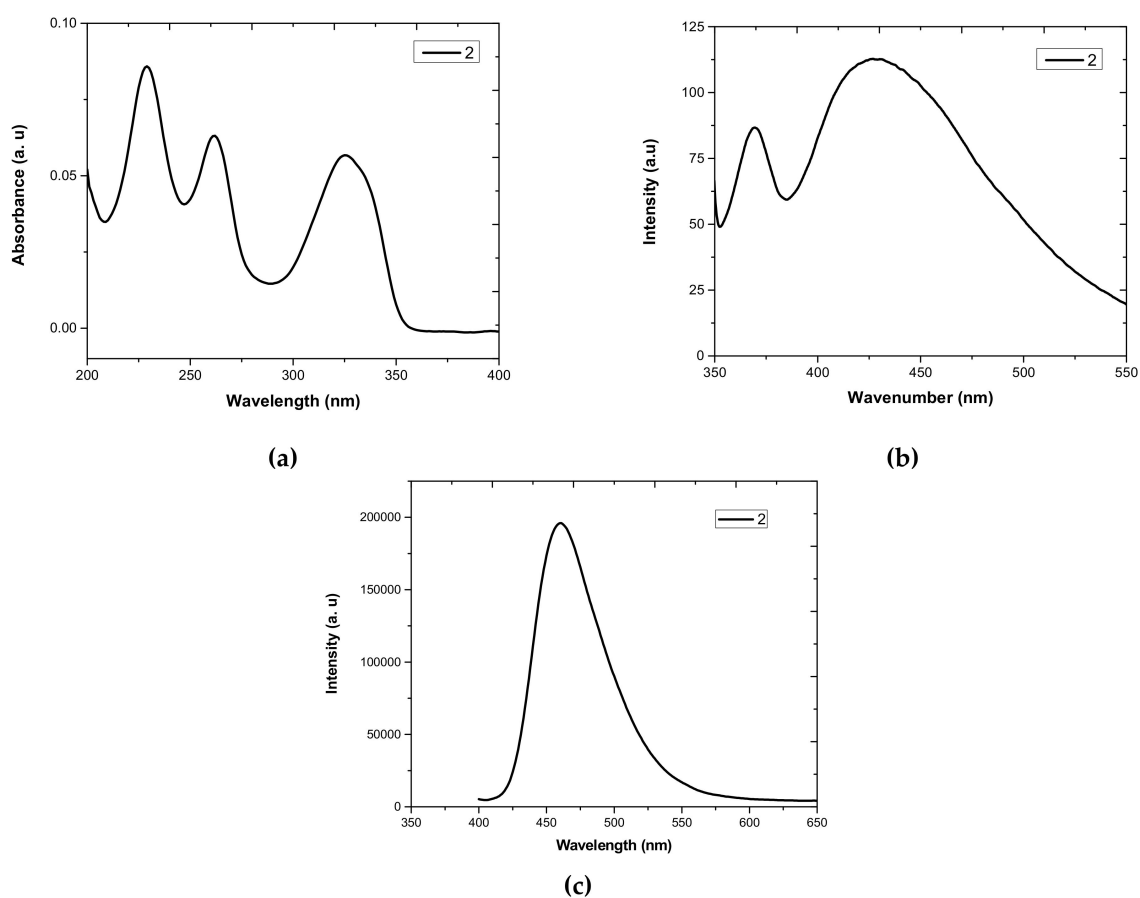


Figure 1. Photophysical properties of ethyl 1-butyl-2-(2-hydroxy-4-methoxyphenyl)-1*H*-benzo[*d*]imidazole-5-carboxylate. (a) UV-Vis absorption spectra of compound 2 in MeCN at room temperature, at 2 μM concentration. (b) Emission spectra of compound 2 in MeCN at room temperature, at 2 μM concentration excited at $\lambda_{\text{exc}} = 326$ nm. (c) Emission spectra of compounds 2 in solid state film when excited at $\lambda_{\text{exc}} = 300$ nm.

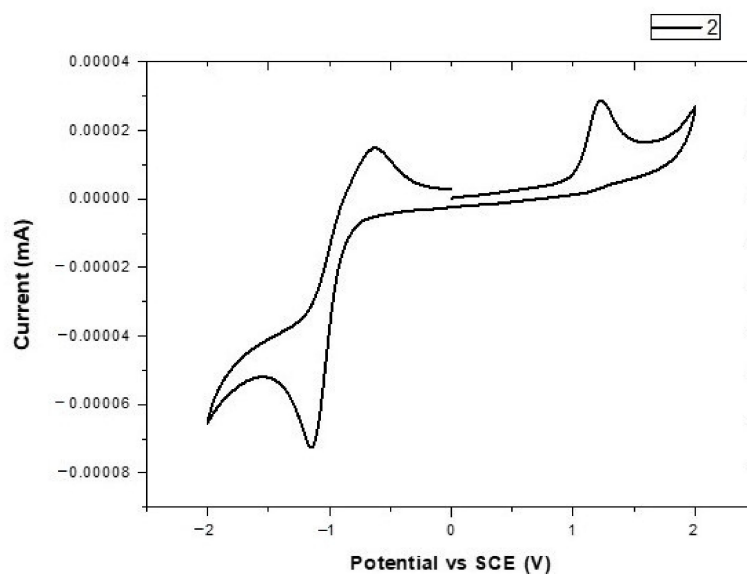


Figure 2. Cyclic voltammograms of compound 2 recorded in MeCN solutions containing 0.1 M tetrabutylammoniumhexafluorophosphate as supporting electrolyte at a scan rate of 100 mV s^{-1} using SCE as the reference electrode, Pt wire as the counter electrode and material-coated glassy carbon as the working electrode.

3.3. Thermal Properties

The thermal property of the new benzimidazole derivatives was determined by thermogravimetric analysis (TGA). The TGA plots are shown in Figure 3. Compound 2 showed a high decomposition temperature (T_d) at 245 °C.

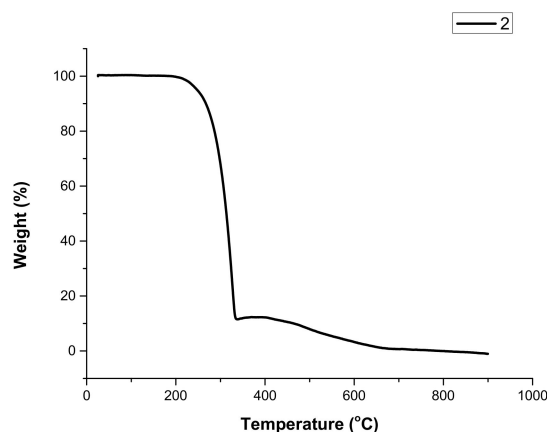


Figure 3. TGA-graph of compound 2.

3.4. Molecular Electrostatic Potential (MEP)

The molecular electrostatic potential (MEP) surface is plotted over the optimized structure (Figure 4) of the synthesized compounds to reveal the sensitivity of a molecule towards electrophilic and nucleophilic attack [26] using a basis set ps-321G, ps-631G and ps-6311G, shown in Figure 4. The MEP generated in the molecule is represented by the different colors. The red color indicates the strongest repulsion and reactivity towards electrophiles, whereas the blue color indicates the strongest attraction and reactivity towards nucleophiles. These results give us evidence about which region of the molecule undergoes intermolecular interaction when the reaction is carried out. It is evident from the figure that the blue color is localized on the carbonyl carbon and hydrogen atoms of the aromatic group, while the red region is localized on the oxygen atom of the ester, methoxy and hydroxyl group.

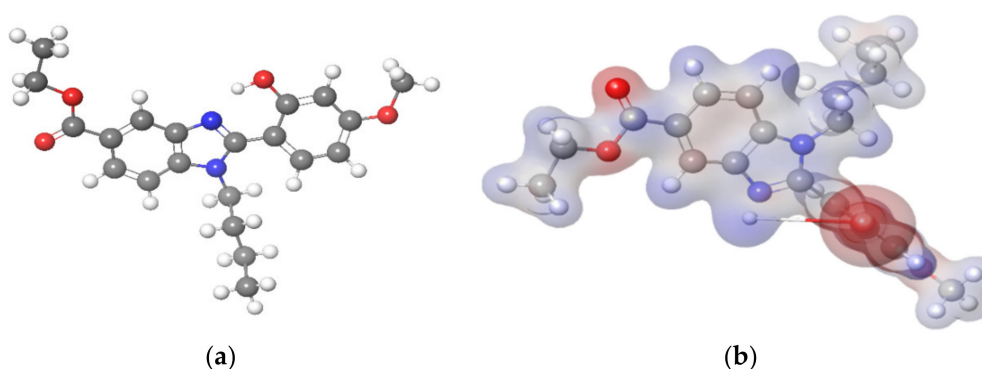


Figure 4. (a) Optimized structure of 2; (b) molecular electrostatic potential (MEP) of compound 2.

4. Materials and Methods

The analytical grade reagents were used for the synthesis of the derivatives, and were purchased from Loba Chem (Mangaluru, India), Spectrochem (Mangaluru, India), and S. D. Fine (Mangaluru, India) without any further purifications. The melting point was determined by the open capillary method and was uncorrected. The confirmation of the title compound was done by ^1H NMR, ^{13}C NMR and COSY spectra in JEOL, JNM-ECZ400/L1 (Tokyo, Japan), 400 MHz. The internal standard used was tetramethylsilane.

The chemical shift values were represented in parts per million (ppm) and Hertz (Hz) for coupling constants. Shimadzu (Shimadzu Corporation, Kyoto, Japan) was used to record FT (ATR)-IR absorption spectra in the range 4000–400 cm^{-1} . Shimadzu LCMS-8030 (Shimadzu Corporation, Kyoto, Japan) was used to record mass spectra and was uncorrected. The completion of the reaction was determined by thin-layer chromatography on a silica-coated aluminum sheet. Ethyl acetate and hexane were used as a mobile phase. The UV-Vis spectra of the derivatives were measured in the MeCN, EtOH, DMF, DMSO and THF solvents (concentration 2 μM) at room temperature using a Shimadzu spectrometer (Shimadzu Corporation, Kyoto, Japan). The photoluminescence (PL) spectra were recorded in a Hitachi, Japan F-7000 Fluorescence Spectrophotometer (Shimadzu Corporation, Kyoto, Japan). The cyclic voltammetry (CV) experiment was conducted in an Ivium vertex electrochemical workstation (Bangalore, India) with 100 mV s^{-1} scan rates. The experiment was performed using a three-electrode cell in MeCN solvent. The 0.1 M solution of tetrabutylammonium hexafluorophosphate in MeCN was used as the supporting electrolyte, standard calomel electrode (SCE) was used as a reference electrode and platinum was used as a counter electrode. The thermogravimetric analysis (TGA) was carried using an STA-2500, NETZSCH, Wittelsbacherstrabe 42, Germany at a heating rate of 10 $^{\circ}\text{C min}^{-1}$ under an inert atmosphere. The density functional theory (DFT) and molecular electrostatic potential (MEP) were assessed using an Acer Veriton i5 Workstation using Materials Science Suite 2017-1, Schrödinger LLC, New York, NY, USA, 2017.

Ethyl 1-butyl-2-(2-hydroxy-4-methoxyphenyl)-1H-benzol[d]imidazole-5-carboxylate (2)

Ethyl 4-chloro-3-nitrobenzoate (**1**) was Prepared According to the Literature [24]. To a stirred solution of ethyl 4-chloro-3-nitrobenzoate (**1**) (0.50 g, 19.8 mmol) in dry DMSO (5.0 mL) at room temperature was added 4-methoxy salicylaldehyde (0.29 g, 19.8 mmol) and sodium dithionite (0.65 g, 39.6 mmol). The stirred mixture was then heated to 90 $^{\circ}\text{C}$ for 3 h. The completion of the reaction was monitored by TLC. The reaction mass was poured into ice-cold water, and the precipitate formed was filtered, dried and recrystallized to afford the title compound **2** (0.6 g, 87%) as an off-white solid, m.p. 110–112 $^{\circ}\text{C}$ (DMF); FT-IR (ATR, $\nu_{\text{max}}/\text{cm}^{-1}$): 3412 (-OH), 1701 (C=O of ester), 1292 (C-O of ester); $^1\text{H-NMR}$ (400 MHz, $\text{DMSO-}d_6$): 0.74 (t, 3H, $J = 7.2$, 4- CH_3), 1.13 (q, 2H, $J = 7.2$, 3- CH_2), 1.36 (t, 3H, $J = 6.8$, ester CH_3), 1.64 (quint, 2H, $J = 7.2$, 2- CH_2), 3.81 (s, 3H, MeO), 4.28 (t, 2H, $J = 6.8$, 1- CH_2), 4.35 (q, 2H, $J = 7.2$, ester CH_3), 6.62 (d, 2H, $J = 8.0$, H_3 and H_5 of 4-OMe-2-hydroxy-phenyl), 7.46 (d, 1H, $J = 8.4$, H_7 of benzimidazole), 7.80 (d, 1H, $J = 8.4$, H_6 of 4-OMe-2-hydroxy-phenyl), 7.95 (1H, $J = 8.4$, H_6 of benzimidazole), 8.26 (s, 1H, H_4 benzimidazole) ppm, OH is absent; $^{13}\text{C NMR}$ (101 MHz, $\text{DMSO-}d_6$): 13.3, 14.3, 19.2, 30.9, 44.2, 55.3, 60.6, 101.4, 105.8, 108.1, 111.0, 119.5, 123.5, 124.1, 131.8, 137.9, 140.2, 153.5, 157.5, 162.2, 166.1 ppm; MS: calculated for $\text{C}_{21}\text{H}_{24}\text{N}_2\text{O}_4$ is 368.17; found $[\text{M} + \text{H}]^+$ 369.15 m/z ; Anal. calc. for $\text{C}_{21}\text{H}_{24}\text{N}_2\text{O}_4$: C, 68.46; H, 6.57; N, 7.60%. Found: C, 68.44; H, 6.53; N, 7.57%; UV-Vis: λ_{max} (MeCN) = 326 nm. Fluorescence: λ_{ex} = 326 nm, λ_{em} (MeCN) = 429 nm, $\Phi = 0.1$.

5. Conclusions

In this study, the synthesis of benzimidazole in a good yield, and its characterization using FTIR, $^1\text{H NMR}$, COSY, $^{13}\text{C-NMR}$, mass spectrometry, UV-Vis, PL, thin-film solid emission spectra, CV and TGA analysis, were reported. Compound **2** exhibited blue emission.

Supplementary Materials: The following are available online, Figure S1: Cyclic voltammogram of ferrocence, Figure S2: Uv-Vis and PL of 2-naphthylamine, Figure S3: FT-IR Spectrum, Figure S4–S7: $^1\text{H NMR}$ spectrum, Figure S8–S10: $^{13}\text{C NMR}$ Spectrum, Figure S11: COSY spectrum, Figure S12: Mass spectrum.

Author Contributions: Experiments, writing—original draft preparation and formal analysis, R.S.; Supervision, B.P. All authors have read and agreed to the published version of the manuscript.

Funding: This research was funded by DST/KSTePS through fellowship.

Data Availability Statement: The data presented in this study are available in Supplementary Materials.

Acknowledgments: The author R.S. thanks DST/KSTePS, Karnataka for providing Ph.D. Fellowship. The authors are thankful to DST-PURSE Laboratory, Mangalore University, CeNS Bangalore for analytical data and Department of Biochemistry, Mangalore University for computational studies.

Conflicts of Interest: The authors have no conflicts of interest.

Sample Availability: Samples of the compounds are available from the authors.

References

1. Paramashivappa, R.; Kumar, P.P.; Rao, P.S.; Rao, A.S. Design, synthesis and biological evaluation of benzimidazole/benzothiazole and benzoxazole derivatives as cyclooxygenase inhibitors. *Bioorg. Med. Chem. Lett.* **2003**, *13*, 657–660. [[CrossRef](#)]
2. Achar, K.C.; Hosamani, K.M.; Seetharamareddy, H.R. In-vivo analgesic and anti-inflammatory activities of newly synthesized benzimidazole derivatives. *Eur. J. Med. Chem.* **2010**, *5*, 2048–2054. [[CrossRef](#)] [[PubMed](#)]
3. Karthikeyan, C.; Solomon, V.R.; Lee, H.; Trivedi, P. Synthesis and biological evaluation of 2-(phenyl)-3H-benzo [d] imidazole-5-carboxylic acids and its methyl esters as potent anti-breast cancer agents. *Arab. J. Chem.* **2017**, *10*, S1788–S1794. [[CrossRef](#)]
4. Kwak, H.J.; Pyun, Y.M.; Kim, J.Y.; Pagire, H.S.; Kim, K.Y.; Kim, K.R.; Dal Rhee, S.; Jung, W.H.; Song, J.S.; Bae, M.A.; et al. Synthesis and biological evaluation of aminobenzimidazole derivatives with a phenylcyclohexyl acetic acid group as anti-obesity and anti-diabetic agents. *Bioorg. Med. Chem. Lett.* **2013**, *23*, 4713–4718. [[CrossRef](#)]
5. Klimesova, V.; Koci, J.; Pour, M.; Stachel, J.; Waisser, K.; Kaustova, J. Synthesis and preliminary evaluation of benzimidazole derivatives as antimicrobial agents. *Eur. J. Med. Chem.* **2002**, *37*, 409–418. [[CrossRef](#)]
6. Kus, C.; Ayhan-Kilcigil, G.; Ozbey, S.; Kaynak, F.B.; Kaya, M.; Çoban, T.; Can-Eke, B. Synthesis and antioxidant properties of novel N-methyl-1, 3, 4-thiadiazol-2-amine and 4-methyl-2H-1, 2, 4-triazole-3 (4H)-thione derivatives of benzimidazole class. *Bioorg. Med. Chem.* **2008**, *16*, 4294–4303. [[CrossRef](#)] [[PubMed](#)]
7. Kundu, N.; Audhya, A.; Abtab, S.M.T.; Ghosh, S.; Tiekink, E.R.; Chaudhury, M. Anion-controlled assembly of silver (I) complexes of multiring heterocyclic ligands: A structural and photophysical study. *Cryst. Growth Des.* **2010**, *10*, 1269–1282. [[CrossRef](#)]
8. Huang, W.K.; Wu, H.P.; Lin, P.L.; Lee, Y.P.; Diau, E.W.G. Design and Characterization of Heteroleptic Ruthenium Complexes Containing Benzimidazole Ligands for Dye-Sensitized Solar Cells: The Effect of Fluorine Substituents on Photovoltaic Performance. *J. Phys. Chem. Lett.* **2012**, *3*, 1830–1835. [[CrossRef](#)]
9. Vijayan, N.; Balamurugan, N.; Babu, R.R.; Gopalakrishnan, R.; Ramasamy, P. Growth and characterization studies of organic NLO crystals of benzimidazole by melt technique. *J. Cryst. Growth.* **2005**, *275*, 1895–1900. [[CrossRef](#)]
10. Singh, N.; Jang, D.O. Benzimidazole-based tripodal receptor: Highly selective fluorescent chemosensor for iodide in aqueous solution. *Org. Lett.* **2007**, *9*, 1991–1994. [[CrossRef](#)]
11. Wu, Y.C.; You, J.Y.; Jiang, K.; Wu, H.Q.; Xiong, J.F.; Wang, Z.Y. Novel benzimidazole-based ratiometric fluorescent probes for acidic pH. *Dyes Pigm.* **2018**, *149*, 1–7. [[CrossRef](#)]
12. Behera, S.K.; Sadhuraragi, G.; Elumalai, P.; Sathiyendiran, M.; Krishnamoorthy, G. Exclusive excited state intramolecular proton transfer from a 2-(2'-hydroxyphenyl) benzimidazole derivative. *RSC Adv.* **2016**, *6*, 59708–59717. [[CrossRef](#)]
13. Douhal, A.; Amat-Guerri, F.; Lillo, M.P.; Acuna, A.U. Proton transfer spectroscopy of 2-(2'-hydroxyphenyl) imidazole and 2-(2'-hydroxyphenyl) benzimidazole dyes. *J. Photoch. Photobio. A* **1994**, *78*, 127–138. [[CrossRef](#)]
14. Padalkar, V.S.; Ramasami, P.; Sekar, N. A combined experimental and DFT-TDDFT study of the excited-state intramolecular proton transfer (ESIPT) of 2-(2'-hydroxyphenyl) imidazole derivatives. *J. Fluoresc.* **2013**, *23*, 839–851. [[CrossRef](#)] [[PubMed](#)]
15. Sontakke, V.A.; Kate, A.N.; Ghosh, S.; More, P.; Gonnade, R.; Kumbhar, N.M.; Kumbhar, A.A.; Chopade, B.A.; Shinde, V.S. Synthesis, DNA interaction and anticancer activity of 2-anthryl substituted benzimidazole derivatives. *New J. Chem.* **2015**, *39*, 4882–4890. [[CrossRef](#)]
16. Ma, S.; Fu, Y.; Ni, D.; Mao, J.; Xie, Z.; Tu, G. Spiro-fluorene based 3D donor towards efficient organic photovoltaics. *Chem. Commun.* **2012**, *48*, 1187–11849. [[CrossRef](#)]
17. Nie, J.; Li, N.; Ni, Z.; Zhao, Y.; Zhang, L. A sensitive tetraphenylethene-based fluorescent probe for Zn²⁺ ion involving ESIPT and CHEF processes. *Tetrahedron Lett.* **2017**, *58*, 1980–1984. [[CrossRef](#)]
18. Yuen, J.D.; Fan, J.; Seiffter, J.; Lim, B.; Hufschmid, R.; Heeger, A.J.; Wudl, F. High performance weak donor–acceptor polymers in thin film transistors: Effect of the acceptor on electronic properties, ambipolar conductivity, mobility, and thermal stability. *J. Am. Chem. Soc.* **2011**, *133*, 20799–20807. [[CrossRef](#)] [[PubMed](#)]
19. Gornn, P.; Lehnhardt, M.; Kowalsky, W.; Riedl, T.; Wagner, S. Elastically Tunable Self-Organized Organic Lasers. *Adv. Mater.* **2011**, *23*, 869–872. [[CrossRef](#)]
20. Qin, W.; Lam, J.W.; Yang, Z.; Chen, S.; Liang, G.; Zhao, W.; Kwok, H.S.; Tang, B.Z. Red emissive AIE luminogens with high hole-transporting properties for efficient non-doped OLEDs. *Chem. Commun.* **2015**, *51*, 7321–7324. [[CrossRef](#)] [[PubMed](#)]
21. Huang, J.; Sun, N.; Dong, Y.; Tang, R.; Lu, P.; Cai, P.; Li, Q.; Ma, D.; Qin, J.; Li, Z. Similar or totally different: The control of conjugation degree through minor structural modifications, and deep-blue aggregation-induced emission luminogens for non-doped OLEDs. *Adv. Funct.* **2013**, *23*, 2329–2337. [[CrossRef](#)]

22. Chen, L.; Lin, G.; Peng, H.; Nie, H.; Zhuang, Z.; Shen, P.; Ding, S.; Huang, D.; Hu, R.; Chen, S.; et al. Dimesitylboryl-functionalized tetraphenylethene derivatives: Efficient solid-state luminescent materials with enhanced electron-transporting ability for nondoped OLEDs. *J. Mater. Chem. C* **2016**, *4*, 5241–5247. [[CrossRef](#)]
23. Zhang, T.; Zhang, R.; Zhao, Y.; Ni, Z. A new series of N-substituted tetraphenylethene-based benzimidazoles: Aggregation-induced emission, fast-reversible mechanochromism and blue electroluminescence. *Dyes Pigm.* **2018**, *148*, 276–285. [[CrossRef](#)]
24. Vasantha, K.; Basavarajaswamy, G.; Rai, M.V.; Boja, P.; Pai, V.R.; Shruthi, N.; Bhat, M. Rapid 'one-pot' synthesis of a novel benzimidazole-5-carboxylate and its hydrazone derivatives as potential anti-inflammatory and antimicrobial agents. *Bioorg. Med. Chem. Lett.* **2015**, *25*, 1420–1426. [[CrossRef](#)] [[PubMed](#)]
25. Lewis, F.D.; Hougland, J.L.; Markarian, S.A. Formation and Anomalous Behavior of Aminonaphthalene–Cinnamonnitrile Exciplexes. *J. Phys. Chem. A* **2000**, *104*, 3261–3268. [[CrossRef](#)]
26. Tamer, O.; Tamer, S.A.; Idil, O.; Avci, D.; Vural, H.; Atalay, Y. Antimicrobial activities, DNA interactions, spectroscopic (FT-IR and UV-Vis) characterizations, and DFT calculations for pyridine-2-carboxylic acid and its derivatives. *J. Mol. Struct.* **2018**, *1152*, 399–408. [[CrossRef](#)]